Influence of the Heme Pocket Conformation on the Structure and Vibrations of the Fe-CO Bond in Myoglobin: A QM/MM Density Functional Study

Carme Rovira,* Brita Schulze,† Markus Eichinger,‡ Jeffrey D. Evanseck,† and Michele Parrinello§
*Departament de Química Física, Universitat de Barcelona, 08028 Barcelona, Spain; †Department of Chemistry, University of Miami, Coral Gables, Florida 33146 USA; ‡JOMESA Messysteme GmbH, 80335 München, Germany; and §Max-Planck-Institut für Festkörperforschung, 70569 Stuttgart, Germany

ABSTRACT The influence of the distal pocket conformation on the structure and vibrations of the heme-CO bond in carbonmonoxy myoglobin (MbCO) is investigated by means of hybrid QM/MM calculations based on density functional theory combined with a classical force field. It is shown that the heme-CO structure (QM treated) is quite rigid and not influenced by the distal pocket conformation (MM treated). This excludes any relation between FeCO distortions and the different CO absorptions observed in the infrared spectra of MbCO (A states). In contrast, both the CO stretch frequency and the strength of the CO···His64 interaction are very dependent on the orientation and tautomerization state of His64. Our calculations indicate that the CO···N_ϵ type of approach does not contribute to the A states, whereas the CO···H-N_ϵ interaction is the origin of the A_1 and A_3 states, the His64 residue being protonated at N_ϵ. The strength of the CO···His64 interaction is quantified, in comparison with the analogous O_2···His64 interaction and with the observed changes in the CO stretch frequency. Additional aspects of the CO···His64 interaction and its biological implications are discussed.

INTRODUCTION

Myoglobin (Mb), a small globular protein that stores oxygen in muscles, has often served as an example of ligand binding, control, and recognition (Stryer, 1995). The binding of oxygen (O_2) and carbon monoxide (CO) to the heme active center is a complex process determined by many structural and dynamic properties of both the heme active center and the surrounding protein. Many essential aspects of this function, such as the way the protein controls the binding of ligands, are a topic of debate (Sage and Champion, 1996; Springer et al., 1994; Olson and Phillips, 1996).

The structural and vibrational properties of the Fe-CO moiety are commonly used as a sensitive probe for electrostatic interactions in the distal pocket (Quillin et al., 1994; Ray et al., 1994; Unno et al., 1998; Phillips et al., 1999). The bound CO ligand exhibits four main infrared (IR) absorption bands, denoted A_0, A_1, and A_3, with vibrational frequencies $\nu(A_0) \approx 1965\ cm^{-1}$, $\nu(A_1) \approx 1949\ cm^{-1}$, and $\nu(A_3) \approx 1933\ cm^{-1}$. Moreover, a recent IR study (Müller et al., 1999) introduced an additional state, denoted A_x, blue-shifted by 4 cm^{-1} from A_0. These absorptions, which change relative intensity and wavenumber depending on temperature, pressure, pH, or solvent (Fuchsman and Appleby, 1979; Shimada and Caughey, 1982; Ansari et al., 1987; Hong et al., 1990; Iben et al., 1989; Morikis et al., 1989; Frauenfelder et al., 1990; Zhu et al., 1992; Mourant et al., 1993; Müller et al., 1999), are used to identify functionally different conformational substates of MbCO called taxonomic substates (Johnson et al., 1996; Frauenfelder et al., 1991; Nienhaus and Young, 1996). However, the relation between the A states and specific structural features of the protein has not yet been clarified.

The A_0 component is observed upon lowering the pH or mutating the distal histidine residue (His64) (Quillin et al., 1994; Li et al., 1994; Braunstein et al., 1993; Springer et al., 1994). The x-ray study of MbCO at low pH (Yang and Phillips, 1996) has demonstrated that His64 is far from the ligand and out of the heme pocket. Thus, the A_0 state has often been associated with the CO being in an apolar environment.

The structural origin of the A_1 and A_3 states is less clear. It was proposed early on that they correspond to different degrees of distortion of the FeCO unit caused by steric interactions in the heme pocket (Yu et al., 1983; Ormos et al., 1988). This was supported by the fact that neutron and x-ray structures show that the FeCO bond is far from linear (Cheng and Schoenborn, 1991; Yang and Phillips, 1996). Because large CO distortions would weaken the Fe-CO bond, a relation was assumed between A states and protein CO discrimination. However, the quite large distortions reported in x-ray studies have been challenged (see for instance Ray et al., 1994; Slebodnick and Ibers, 1997). Spectroscopic studies (Lim et al., 1995; Sage and Jee, 1997) have given a much smaller distortion ($\sim 7^o$ deviation from linearity), and theoretical calculations have demonstrated that the energetic cost for such a small deformation is marginal (Vangberg et al., 1997; Rovira et al., 1997; Spiro

Received for publication 17 October 2000 and in final form 16 March 2001.

B. Schulze's current address: MBT Munich Biotechnology GmbH, Fraunhoferstrasse 10, 82152 Martinsried, Germany.

J. D. Evanseck's current address: Department of Chemistry and Biochemistry, Duquesne University, 600 Forbes Avenue, Pittsburgh, PA 15282.

Address reprint requests to Dr. Carme Rovira, Universitat de Barcelona, Departament de Química Física, Marti i Franques 1, 08028 Barcelona, Spain. Tel.: 34-93-402-1228; Fax: 34-93-402-1231; E-mail: c.rovira@qf.ub.es.

0006-3495/01/07/435/11 $2.00

and Kozlowski, 1998; Havlin et al., 1998). Nevertheless, the role of steric factors in CO discrimination is still supported by some authors (Collman, 1997; Kachalova et al., 1999).

On the other hand, a number of spectroscopic studies support the hypothesis that it is the polarity of the heme pocket that determines the ligand vibrations (Unno et al., 1998; Ray et al., 1994; Springer et al., 1994; Li et al., 1994; Phillips et al., 1999). In particular, it is assumed that the A states arise from different rotational conformations and/or tautomerization states of the distal histidine (Fig. 1) (Jewsbury and Kitagawa, 1994; Schulze and Evanseck, 1999; Vojtechovsky et al., 1999). However, the correspondence between the A states and specific His64 conformations is very controversial. One of the main difficulties comes from the fact that the tautomerization state of His64 is unclear. The early neutron structure of MbCO suggested that His64 is protonated at N_δ with the N_ϵ lone pair pointing toward the CO (Cheng and Schoenborn, 1991). However, other experimental studies propose that His64 is protonated at N_ϵ (Unno et al., 1998; Phillips et al., 1999), which is in analogy with MbO_2 (Phillips and Schoenborn, 1981) and MbCN (Bhattacharya et al., 1997).

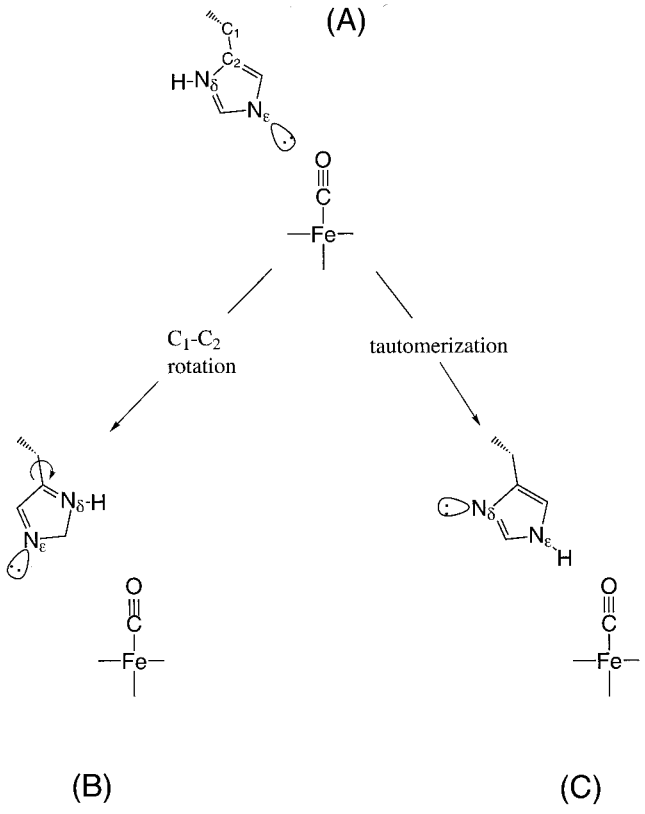

FIGURE 1 Types of CO···His64 approaches originated by either His64 rotation around the C_1-C_2 bond or by a tautomerization change. The starting configuration (*a*) is the one given by the neutron structure of MbCO. This configuration has been associated with A_3 (Ray et al., 1994) or A_1 (Vojtechovsky et al., 1999). Configuration *b* has been proposed to be A_3 (Oldfield et al., 1991; Kushkuley and Starov, 1997) as well as A_1 (Jewbury and Kitagawa, 1994). Configuration *c* has been associated with either A_1 (Oldfield et al., 1991; Kushkuley and Starov, 1997), A_3 (Vojtechovsky et al., 1999; Jewsbury and Kitagawa, 1994; Sigfridson and Ryde, 1999) or both A_1 and A_3 (Nienhaus et al., 1997).

The structural origin of the A states has also been studied with theoretical methods. Molecular dynamics (MD) simulations have highlighted the easy rotation and swinging out motion of the His64 residue (Jewsbury and Kitagawa, 1994; Schulze and Evanseck, 1999). Electrostatic models have predicted the effect of these motions on the CO stretch frequency (Oldfield et al., 1991), and quantum mechanical studies have quantified the changes in ν_{CO} (Kushkuley and Starov, 1997; Sigfridson and Ryde, 1999; Cui and Karplus, 2000). Nevertheless, the structural origin of the A states remains controversial, as different studies have given very different interpretations (Fig. 1).

All the above studies were based on either a quantum mechanical treatment on a small heme model or a force-field description on the whole protein. A step forward with respect to this would be to combine a quantum chemical description of the active center and a force-field treatment of the rest of the protein. This would allow us to account together for the interactions of the ligand with the protein backbone (which is expected be of electrostatic and/or steric nature) and the electronic effects at the active center. Moreover, this type of calculation is now feasible with the development of efficient QM/MM methods based on density functional theory.

Here we will apply our recently developed QM/MM method (Eichinger et al., 1998) to investigate the influence of the heme pocket conformation on the structure and vibrations of the Fe-CO bond in MbCO. This study is part of our investigation into the ligand-binding properties of Mb (Rovira et al., 1997, 1999, 2000). Our first objective is to quantify the existence of structural changes in the active center (particularly in the Fe-CO fragment) due to the distal pocket conformation. Our second objective is to determine which conformations can contribute to the A states by calculating the shift of the CO stretching frequency with respect to an unperturbed heme-CO system. It will be shown that, although the structure of the heme is quite robust and not affected by interactions in the distal side, both the CO stretch frequency and the energy of the CO···His64 interaction are very dependent on the conformation of the His64 residue. To the best of our knowledge this is the first study in which these problems are addressed by means of first-principles methods that fully take into account the influence of the whole protein.

COMPUTATIONAL METHOD

The QM/MM calculations were performed using the EGO-CPMD software (Eichinger et al., 1998), which combines a first-principles method based on density functional theory (DFT; Car-Parrinello molecular dynamics (CPMD)) with a force-field molecular dynamics method. The system is partitioned into a QM fragment and an MM fragment. The dynamics of the

atoms on the QM fragment depends on the electronic density, $\rho(r)$, computed with DFT, whereas that of the atoms on the MM fragment is ruled by semi-empirical determined force fields that parameterize molecular forces with harmonic potentials. The CHARMM all-atom parameter set (MacKerell et al., 1998) was used, as implemented in the EGO-VII program. Electrostatic interactions on the MM fragment are treated with a combined structure-adapted multipole method and multiple time step algorithm (Eichinger et al., 1997) to efficiently calculate electrostatic forces so that no cutoff has to be employed. In addition, there are coupling terms that account for the interaction between the two fragments. The QM-MM boundary is treated with the scaled position link atom method (SPLAM). Covalent bonds (C-C) at the boundary were substituted by C-H···C bonds (H = link atom). Further details on the QM/MM methodology used here can be found in Eichinger et al. (1998). This methodology has been proven to describe successfully the structural and energetic properties of several small systems such as the water dimer, an ethane molecule, a simplified retinal shift base, and liquid water (Eichinger et al. 1998). In particular, it was shown to reproduce the harmonic vibration results obtained from the full quantum calculation. It has also been recently applied to characterize the intermediates of the catalytic cycle of galactose oxidase (Röthlisberger et al., 2000).

The calculations including the protein environment used the following QM-MM partition (see Fig. 2). The porphyrin (methyl substituted), the imidazole of His93, and the ligand (CO or O_2) were included in the QM fragment. This option was chosen in the light of our previous results for heme models, where it was found that the axial imidazole substantially enhances the binding energy of the CO and O_2 ligands, whereas the heme vinyl and propionates do not influence their ligand-binding properties (Rovira et al., 1997, 1999, 2000). Thus, only the protein residues that are covalently attached to the heme (His93) were treated quantum mechanically. The rest of the protein residues, whose effect on the heme-ligand bonding were of an electrostatic and/or steric nature, were considered in the MM region. Moreover, inclusion of more residues on the QM region would increase exceedingly the computational overload. The protein was additionally enveloped in a 37-Å sphere of equilibrated TIP3P water molecules so as to take into account solvation effects.

The QM fragment was enclosed in an isolated supercell of dimensions $a = b = 15$ Å, and $c = 10$ Å. The electronic wave functions were expanded in plane waves up to a kinetic energy cutoff of 70 Ry. Martins-Troullier norm-conserving pseudopotentials were used (Troullier and Martins, 1991), supplemented with nonlinear core corrections for the Fe atom (Louie et al., 1982). We used the generalized gradient-corrected approximation, following the prescription of Becke and Perdew (Becke, 1986; Perdew, 1986). This is the same setup as we used for the study of structural and equilibrium properties of heme models (Rovira et al., 1997, 1999, 2000). Interaction energies between the heme and the His64 residue were calculated using the more recent exchange-correlation functional proposed by Perdew et al. (1996), which has been found to be superior than BP for the description of hydrogen bond interactions (Montanari et al., 1999). Nevertheless, binding energies computed with both functionals were sim-

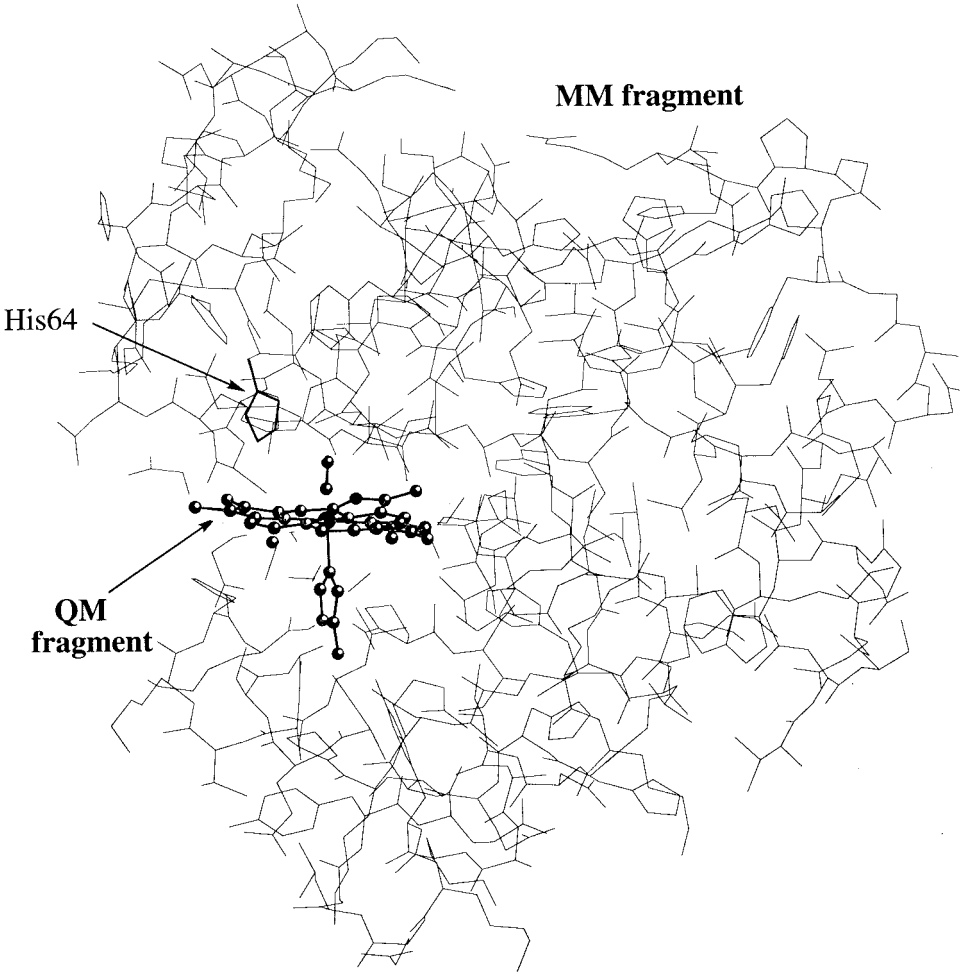

FIGURE 2 QM-MM partition chosen for our calculations. The protein is further surrounded by a shell of water molecules (see text).

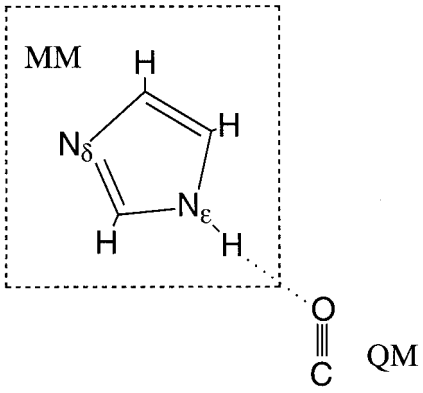

SCHEME 1

ilar and did not affect the interpretation of our data. For a detailed description of the CPMD method, see Car and Parrinello (1985) and Galli and Parrinello (1991).

Due to its large computational cost, simultaneous optimization of the QM (63 atoms) and MM fragments (20,000 atoms) is not feasible. Thus, we optimized only the structure of the QM fragment for each of the structures, while keeping the protein environment (MM fragment) fixed. This is not expected to be a severe approximation so long as our initial structures are carefully selected (see below).

Harmonic ligand stretch frequencies were computed from the diagonalization of the Hessian matrix obtained by numerical energy derivatives. The Fe atom, its neighboring nitrogen atoms (four N atoms of the porphyrin and the N of the axial imidazole), and the CO ligand were included in the Hessian matrix. Test calculations showed that this set of atoms is sufficient to obtain ligand-stretching frequencies in agreement with the full Hessian calculation. A finite step size of 0.01 Å was taken for the ionic displacements, and the energy was converged up to 10^{-6} a.u. The reference structure for the frequency calculation was taken as the isolated QM fragment. Frequency shifts ($\Delta\nu_{CO}$ and $\Delta\nu_{FeC}$) are referred to as differences with respect to the CO stretch frequency of the reference structure. The effect of a given protein residue (e.g., Arg45 or His97) on $\Delta\nu_{CO}$ was evaluated by switching to zero the coulomb and van der Waals parameters for that particular residue and re-optimizing the structure of the QM fragment. Although the absolute frequencies we obtain can be off by several cm^{-1}, the computed shifts should be accurate enough to account for the trends among different protein conformations. We estimate the accuracy of the shifts on the computed vibrational frequencies to be less than 3 cm^{-1}.

Preliminary test calculations were performed on a small model built from a CO molecule interacting with an imidazole ring (see Scheme I). The imidazole was oriented such that a CO···H-N_ϵ interaction takes place, with an O···H distance of 1.70 Å. The CO and imidazole were taken as QM and MM fragments, respectively. The shift of the CO vibrational frequency in the presence of the imidazole donor ($\Delta\nu_{CO} = -22$ cm^{-1}) reproduces fairly well the value obtained in the full quantum calculation ($\Delta\nu_{CO} = -21$ cm^{-1}).

RESULTS AND DISCUSSION

Initial structures

The initial structures for the QM/MM computations were taken from two sources: 1) the neutron diffraction structure and 2) snapshots from previous force-field MD simulations using the same MM setup (Schulze and Evanseck, 1999).

The neutron diffraction structure assigned a proton to the N_δ of His64, forming a CO···N_ϵ type of interaction (Fig. 1 *a*). The FeCO fragment is quite distorted in the two refined positions (⟨FeCO = 145.8°/135.2°) and the distance between N_ϵ and the carbonyl oxygen is 3.48/2.60 Å. As mentioned in the Introduction, the tautomerization state of His64 is very controversial. Thus, an additional structure was prepared by changing the position of the N_δ proton so as to generate the N_δ tautomer with a CO···H-N_ϵ interaction (Fig. 1 *c*). This allows us to quantify the changes in the Fe-ligand properties due to the tautomerization state of His64. All other protein residues were kept at the same position in both cases.

Another set of initial structures was selected from snapshots of previous MD simulations (Schulze and Evanseck, 1999) using the CHARMM force field, starting from the x-ray structure of Kuriyan et al. (1986) at 1.5-Å resolution. The type of CO···His64 approach in each of the selected protein conformations is shown in Fig. 3. Interestingly, a simulation using the N_δ tautomer led to rotation of the His64 residue (I→III). We took a snapshot from each of the two rotational conformations (occurring at 60 ps and 128 ps of the simulation), in which the ligand interacts either with the unprotonated nitrogen (I: CO···N_ϵ) or with the protonated one (III: CO···H-N_δ). Another MD snapshot (II) was taken from a simulation using the N_ϵ tautomer (Schulze, 1999). In this case, no rotation of the His64 imidazole was observed during the simulation, and the CO···H-N_ϵ interaction remained. The same protein configuration after inducing an artificial 180° rotation of the His64 imidazole (IV) was also considered. Finally, we took a fifth MD snapshot (V) in which the His64 residue moved away from the ligand (6 Å from the closest nitrogen atom).

Optimized structures

We started our study by performing a QM/MM calculation on the protein structure given by the neutron diffraction data. Table 1 lists the main structural parameters obtained by the optimization (see Computational Method). The local structure around the Fe atom changes substantially with respect to the neutron diffraction structure. The CO and Fe-C distances decrease to values that are very similar to those of an isolated heme-CO model (Rovira et al., 1997). The Fe-N_ϵ distance decreases by 0.14 Å, and the distortion of the FeCO from linearity is much less pronounced: the FeCO angle increases from 145.8°/135.2° to 169°, i.e., only 11° of deviation from the ideal linear bond. This small remaining distortion is probably induced by the strain present in the neutron diffraction structure (note also that there is a sizable tilt of FeCO). An additional calculation deleting the His64 residue from the neutron structure shows that the linearity of the CO is practically restored (FeCO = 176°). This indicates that, independently of the tautomerization state of His64, a sufficiently small heme pocket is

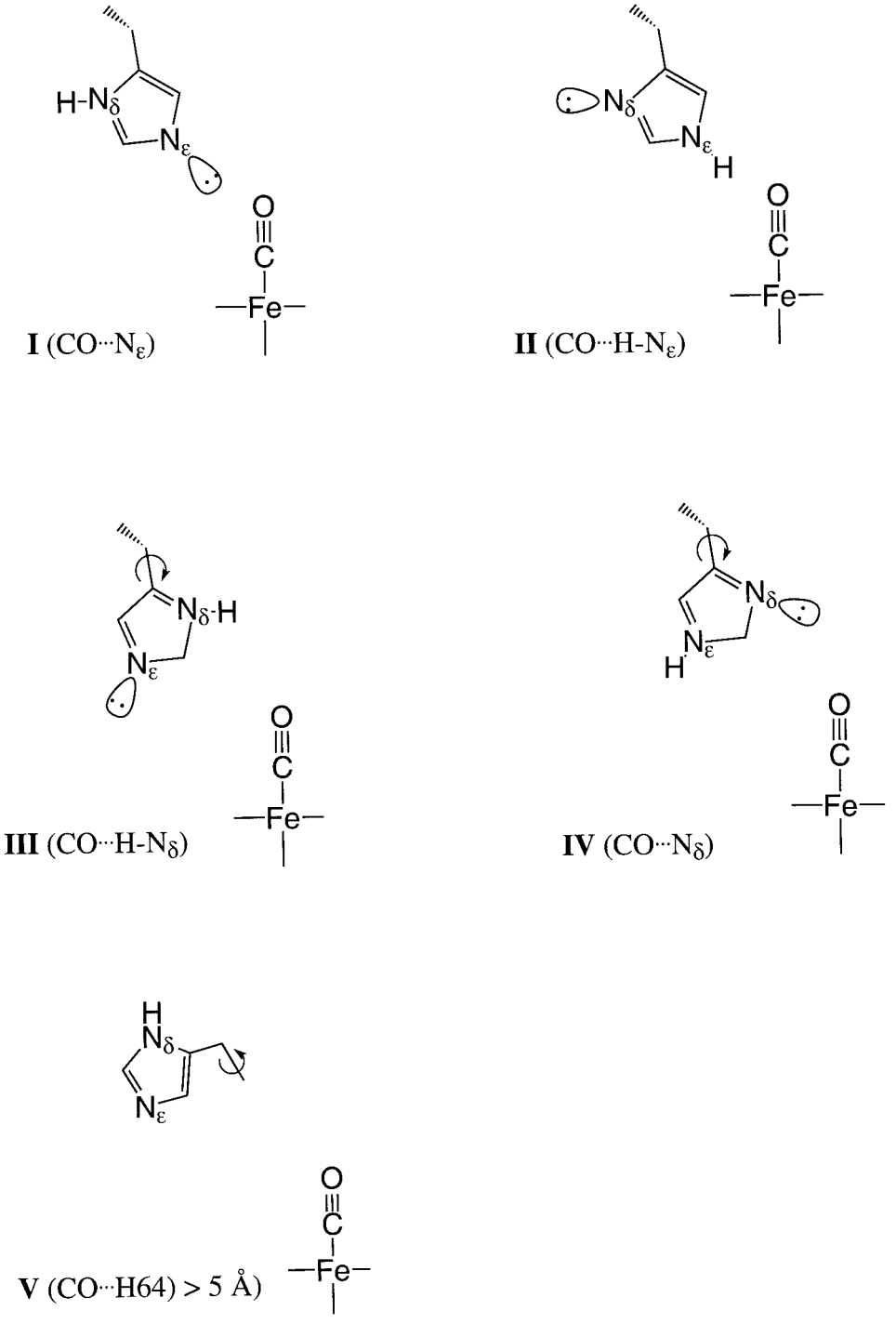

FIGURE 3 Different types of CO···His64 approaches in the selected protein configurations. Each configuration corresponds to a different rotational and/or tautomerization state of the His64 residue. Configurations I, III, and IV correspond to the same MD trajectory at 60 ps (I), 128 ps (II), and 700 ps (III).

able to exert enough steric interaction to distort the FeCO bond slightly. Nevertheless, such a small distortion of the FeCO angle (11°) is not expected to weaken significantly the CO bond (Ghost and Bocian, 1996; Rovira et al., 1997). The significant differences between computation and experiments for the local structure around the iron atom (Table 1) will be discussed in the next section.

Another set of calculations was performed starting from snapshots of previous MD simulations using the EGO software (Schulze and Evanseck, 1999). This corresponds to a more realistic choice than using directly the neutron structure, which is essentially an average among many instantaneous protein configurations. The equilibrated protein structure is free of the strain present in the neutron diffraction

TABLE 1 Main parameters defining the optimized heme-CO structure of each protein conformation considered

Structure	Interaction type	O···X (Å)	C–O (Å)	Fe–C (Å)	θ_{FeCO} (degrees)	δ_{FeCO} (Å)	Fe–N_p (Å)	Fe–N_ε (Å)
Experiment*	CO···N_ϵ	3.48/2.60	1.21/1.19	2.12	145.8/135.2	9.7	2.02	2.26
Calculated	CO···N_ϵ	2.92	1.16	1.74	168.6	6.8	2.00–2.05	2.12
Calculated	CO···H–N_ϵ	2.12	1.17	1.72	168.8	7.0	2.03–2.05	2.12

*Neutron diffraction structure (Cheng and Schoenborn, 1991).

structure, which could indirectly influence the heme pocket conformation. As described above, the snapshots selected for our calculations are characterized by having different conformations of the His64 residue (Fig. 3). Table 2 lists the main structural parameters obtained from the QM/MM optimization of each protein structure (I–V in Fig. 3). Despite having small differences in the porphyrin deformation (not shown here), the iron-ligand structure is not affected by this. This insensitivity with respect to porphyrin deformations was also noticed in our study of the picket-fence porphyrin (Rovira and Parrinello, 1999). Moreover, the different distal pocket conformations do not change the local structure around the Fe atom, which remains close to that of an isolated heme-CO system (last row in Table 2). Interestingly, the FeCO bond is practically linear in all cases, the maximum deformation being of 4°. Together with the results obtained using the neutron diffraction structure (see above), our calculations rule out that the FeCO distortion can be responsible for the observed A states. It seems very improbable from our calculations that the heme pocket conformation would be able to deform the FeCO bond significantly. Even in the case of a largely closed pocket such as the one given by the neutron diffraction structure, the deformation of the FeCO angle amounts to less than 12°. Therefore, the local heme structure seems to be quite insensitive to interactions on the distal side. As we will see in the next section, the same is not true for vibrational frequencies.

Ligand stretch frequencies

Table 3 lists the CO stretch frequencies obtained for each of the pocket conformations of Fig. 3. The values in parentheses correspond to the calculation performed using the neutron diffraction structure. As shown in Table 3, the CO stretch frequency appears to be very dependent on the orientation and protonation state of His64. For instance, the conformation with the unprotonated N_ϵ pointing toward the CO ligand (I) upshifts the CO frequency by 14 cm^{-1}, whereas whenever a NH group is close to the ligand the CO frequency is largely downshifted (up to -26 cm^{-1}). The largest downshift (-23, -26 cm^{-1}) is given by the CO···H-N_ϵ interaction (II). In this case, the hydrogen bond is geometrically more favored than in the case of the analogous interaction in the N_δ tautomer (III), for which the downshift is less pronounced (-14 cm^{-1}). The configuration with His64 far from the ligand does not shift the CO frequency significantly. On the other hand, our calculations indicate an inverse correlation between the $\Delta\nu_{CO}$ and $\Delta\nu_{FeC}$ values ($\Delta\nu_{CO}$ increases as $\Delta\nu_{FeC}$ decreases). This general trend has been observed across a wide range of heme proteins and synthetic models (Li and Spiro, 1988; Ray et al., 1994; Vogel et al., 1999; Phillips et al., 1999).

The frequency changes of Table 3 can be rationalized in terms of variations in the Fe-CO back bonding (i.e., the interaction of the *d-Fe* levels with the empty π^*_{CO} orbitals). When a positive charge approaches the CO (such as the proton of His64), the π^*_{CO} orbitals are energetically stabilized. As they get closer in energy to the Fe-d orbitals, the back-bonding increases, and as a consequence, the CO frequency decreases. Thus, a downshifted $\Delta\nu_{CO}$ is observed for the CO···H-N interactions (II, III). In contrast, a negative charge approaching the CO (such as a nitrogen lone pair) would decrease the back-bonding and increase ν_{CO}. In

TABLE 2 Main parameters defining the optimized heme-CO structure of each protein conformation schematized in Fig. 3

Structure	Interaction type	O···X (Å)	C–O (Å)	Fe–C (Å)	θ_{FeCO} (degrees)	δ_{FeCO} (Å)	Fe-N_p (Å)	Fe–N_ϵ (Å)
Experiment	CO···N_ϵ	3.48/2.60	1.21/1.19	2.12	145.8/135.2	9.7	2.02	2.26
I	CO···N_ϵ	3.39	1.16	1.76	177.3	1.2	2.00–2.02	2.09
II	CO···H–N_ϵ	2.69	1.17	1.74	176.1	1.9	1.99–2.02	2.13
III	CO···H–N_δ	3.47	1.16	1.75	179.3	1.8	1.98–2.03	2.10
IV	CO···N_δ	3.90	1.16	1.74	175.7	1.2	1.99–2.02	2.13
	CO···H–C	2.18						
V	CO···N_ϵ	6.03	1.16	1.75	177.6	0.9	1.99–2.03	2.08
	CO···H–C	4.03						
Heme–CO			1.17	1.72	180.0	0.0	2.02	2.08

*Neutron diffraction structure (Cheng and Schoenborn, 1991).

TABLE 3 Shift of the C–O and Fe–C stretch frequencies with respect to the isolated heme-CO system for each of the protein conformations schematized in Fig. 3

Structure	Interaction type	O···X (Å)	$\Delta\nu_{CO}$* (cm^{-1})	$\Delta\nu_{FeC}$ (cm^{-1})	$\Delta E_{O\cdots x}$ (Kcal/mol)
I	CO···N_ϵ	3.39 (2.92)	+14 (+18)	−62	+2.0
II	CO···H–N_ϵ	2.69 (2.12)	−23 (−26)	61	−3.4
III	CO···H–N_δ	3.47	−14	18	−2.5
IV	CO···N_δ	3.90	−4	10	−0.9
	CO···H–C	2.18			
V	CO···N_ϵ	6.03	−1	10	−0.1
	CO···H–C	4.03			
Heme-CO			0	0	

Hydrogen bond energies are also listed.

*It should be noted that the Fe–C stretching and Fe–CO bending appear slightly mixed in most cases. Thus, the values given here include some mixture with Fe–CO bending.

agreement with this argument, an upshift of $\Delta\nu_{CO}$ is obtained for the arrangement I of Fig. 3.

The influence of the heme pocket closeness (i.e., the proximity of all protein residues to the ligand) on $\Delta\nu_{CO}$ can be appreciated by comparing the results obtained on the solution MD structures with those obtained for the much compressed pocket of the neutron diffraction structure (values in parentheses). The shift is slightly larger in the latter case due to the closeness of the heme pocket residues. Nevertheless, we obtain a similar tendency on $\Delta\nu_{CO}$ with the His64 orientation: an upshift for the CO···N_ϵ interaction, a downshift for the CO···H-N_ϵ interaction, and practically no shift when His64 is far from CO. This anticipates the fact that the trends in $\Delta\nu_{CO}$ are mainly a consequence of the His64 position, being independent of the position of the other protein residues.

At that point, one obvious question would be whether His64 is fully responsible for the observed frequency changes. Additional calculations removing this residue from the protein structure showed that the value of ν_{CO} basically recovers that of an isolated heme. There is only a remaining upshift of 2 cm^{-1}, which can be attributed to the protein environment. Together with the sizable $\Delta\nu_{CO}$ values observed for different His64 conformations (Table 3) we conclude that the His64 residue is the main factor responsible for the observed changes in the CO stretch frequency.

As described in the introduction, the CO ligand of MbCO exhibits four main IR absorption frequencies (the A states) whose structural origin is controversial. These absorptions are centered at ~1965 cm^{-1} (A_0), ~1949 cm^{-1} (A_1), and ~1933 cm^{-1} (A_3). The corresponding $\Delta\nu_{CO}$ values with respect to A_0 are 0.0, −16, and −32 cm^{-1}. Taking into account that the A_0 state has been associated with the CO not being perturbed by the environment, there should be a relation between the experimental $\Delta\nu_{CO}$ values and the ones we obtained from the calculation. In fact, from the results of Table 3 we can extract some information as to the structural origin of the A states. First of all, we notice that all experimental $\Delta\nu_{CO}$ values correspond to downshifted frequencies. Therefore, configuration I for which the unprotonated N_ϵ is close to the ligand (as in the neutron diffraction structure) cannot be any of the A states, as we obtain an upshift of $\Delta\nu_{CO}$ in our calculations. This is in agreement with the MD simulations and Hartree-Fock calculations of Schulze and Evanseck (1999) and with recent DFT studies in heme models by Cui and Karplus (2000) and by Sigfridson and Ryde (1999). However, our results are in contrast with other proposed models (Ray et al. 1994; Oldfield et al., 1991; Kachalova et al., 1999). The model of Oldfield et al. was based on the electrical perturbation of the frequency of an isolated CO by the dipole of an interacting imidazole. It was proposed that the A_1 state corresponds to the CO···H-N_ϵ (II in Fig. 3) interaction, whereas A_3 corresponds to conformation III. The discrepancy with our results is likely to be due to the simplicity of the model, which used an empirical expression not taking into account the Fe-CO back bonding. Based on the resonance Raman spectra on Fe(II)-porphyrin models, Ray et al. (1994) proposed that the A_1 substate arise from the N_ϵ tautomer with a CO···H-N_ϵ interaction (II), and the A_3 substate originates from the N_δ tautomer with a CO···N_ϵ interaction (I). However, this interpretation relied on the fact that the conformation given by the neutron diffraction structure (I) is the majority one in crystals.

The recent high-resolution crystal structure of Kachalova et al. (1999) suggests that there is no proton between the epsilon nitrogen and the CO in MbCO (i.e., the CO···N_ϵ interaction is the majority one). The authors justify this interpretation in view of the short C-O bond length (1.12 Å) found, indicating a strong reduction of back bonding caused by the proximity of the N_ϵ lone pair. Another recent high-resolution structure of MbCO (Vojtechovsky et al., 1999) gives a C-O distance even shorter (1.09 Å). These values seem to us extremely short. The gas phase C-O distance is already 1.13 Å, and this distance is expected to elongate when bonded to heme. In fact, we computed a distance of 1.17 Å for CO in the protein, whereas we reproduce well the gas-phase value (Rovira et al., 1997). Our calculations thus

suggest that the C-O distance in MbCO has been often underestimated in x-ray and neutron measurements. As we pointed out in our previous work (Rovira and Parrinello, 2000) an unreasonably short distance for the diatomic ligand (and a longer one for the iron-ligand bond) may arise when considering a purely static point of view for the Fe-ligand bond.

It is also worth pointing out that several recent model calculations agree that the CO···N_ϵ interaction increases the CO stretch frequency. These models range from a CO interacting with an imidazole ring (Schulze and Evanseck, 1999) up to a simplified heme with an interacting imidazole (Sigfridson and Ryde, 1999; Cui and Karplus, 2000). This indicates that the upshift of $\Delta\nu_{CO}$ is an intrinsic property of a CO···N_ϵ interaction, being independent of the presence of other surrounding chemical groups. Therefore, it seems unlikely that this interaction could correspond to one of the A states, as all of them downshift the CO frequency. Even more surprising is the assignment of the CO···N_ϵ interaction as the A_3 state (Ray et al., 1994) because the only pocket conformations with a sizable downshift are those with a N-H donor close to the ligand.

In summary, our results indicate that the CO···N_ϵ interaction does not take place in MbCO and that His64 is not protonated at N_δ. Were that the case, eventual rotation of His64 (due to the relatively weak H-bond formed in the CO···H-N_δ interaction) would lead to a CO···N_ϵ interaction (I in Fig. 3) and to the appearance of an IR band upshifted from A_0, which is something not found in experiments. This brings us to the conclusion that the A_1 and A_3 states originate from the CO···H-N_ϵ interaction, as we obtain a sizable downshift of ν_{CO} for configuration II. Eventual rotation of His64 would lead to conformation (IV) for which $\Delta\nu_{CO}$ is almost as small as the conformation with His64 far from CO (V). It could be that conformation IV contributes to the much less populated A_0 and/or A_x states (Müller et al., 1999) at normal pH.

Concerning the distinction between the A_1 and A_3 states, it has been pointed out (Johnson et al., 1996) that they cannot originate from different His64 tautomers, as the time scale of state interconversion (nanoseconds) is shorter than that of a change in protonation (microseconds). (Note that this has not been taken into account in previous interpretations of the IR spectrum (Oldfield et al., 1991; Li et al., 1994).) In the light of our present results, we cannot make a clear-cut correspondence between these states and specific His64 orientations involving the N_ϵ tautomer. A plausible hypothesis is that they differ in the degree of polarization of His64 induced by a nearby positively charged residue such as Arg45 (Schulze and Evanseck, 1999). (Additional calculations including more protein residues in the QM fragment such as to quantify their interaction with His64 are not possible at present due to its high computational cost.) In fact, additional calculations taking out charged residues near the ligand (such as Arg45 and His97) shows that $\Delta\nu_{CO}$ increases ($+5$ cm^{-1} in the case of Arg45 and $+2$ cm^{-1} for His97). Interestingly, a recent IR study of sperm whale MbCO (Müller et al., 1999) shows that mutation of His97 by an apolar residue (His97F) blue-shifts the CO frequency by $+2$ cm^{-1}. Although our results certainly verify the experimental observation, we should also note that such a small shift is at the limit of our accuracy.

It could also be that the A_1 and A_3 states correspond to different degrees of proximity between His64 and CO originated by steric or electrostatic interactions of His64 with other residues. In this respect, it is worth mentioning that the recent high-resolution x-ray structure of MbCO of Vojtechovsky et al. (1999) found two different positions for the His64 residue. Both of these positions have the N_ϵ close to the CO with occupations of 60% (N_ϵ-O = 3.2 Å) and 20% (N_ϵ-O = 2.7 Å). Assuming that His64 is protonated at N_ϵ, these positions could correspond to A_1 and A_3, respectively.

Energetics of the CO···His64 interaction

To evaluate the interaction between the CO ligand and the His64 residue in each of the configurations of Fig. 3, we isolated the heme-CO and His64 fragment and performed a single-point QM computation. The orientation between the heme-CO fragment and His64 was fixed identical to the one in the protein configuration considered.

Table 3 lists the values obtained for the energy of the CO···His64 interaction. As in the case of vibrational frequencies, the interaction energy is very dependent on the conformation and protonation state of the distal histidine. The configuration with the unprotonated N_ϵ of His64 pointing toward the CO ligand (II) leads to practically no interaction (-0.1 kcal/mol), whereas the interaction is energetically favorable when a protonated nitrogen is close to the ligand. The largest stabilization (-3.4 kcal/mol) is found for the N_ϵ tautomer having a CO···H-N_ϵ interaction, as in this case the geometry is more favorable for hydrogen bonding (see Fig. 3). In the case of the analogous interaction for the N_δ tautomer (CO···H-N_δ), the interaction energy decreases to -2.5 kcal/mol. (Even though the CO···N_ϵ interaction is repulsive, relaxation of the His64 residue in configuration I (Fig. 3) does not move the imidazole ring of His64 much. Probably the combined effect of the whole protein environment keeps the imidazole in its position.) Therefore, the CO···His64 interaction is favorable for all His64 conformations contributing to the A states. This is at variance with the common assumption (Ray et al., 1994) that only O_2 is significantly hydrogen bonded to His64. Our results also differ from previous calculations by Sigfridson and Ryde (1999) using conformations similar to I and II (Fig. 3) but taking directly the neutron diffraction structure. A repulsive CO···His64 interaction was found in both cases. As the authors discuss, it could be that the imprecision of the neutron diffraction structure (the CO is largely bent and disordered into two positions) is the cause of the absence of

hydrogen bonding. On the other hand, our computations support recent resonance Raman measurements (Unno et al., 1998) that show spectroscopic evidence of a hydrogen bond between CO and His64. The combined experimental and computational evidence for hydrogen bonding is in conflict with experimental data for the off rates reported for MbCO (wild type) versus H64L (Springer et al., 1994). The off rates are almost identical, even though hydrogen bond stabilization can be excluded in H64L. Several factors can help rationalize the discrepancy, such as that small energy changes for a single hydrogen bond can have insignificant impact upon off rates. It could also be that the mutation leads to a reorganization of the ligand-binding site and offer new nonbond interactions that compensate for the loss of the hydrogen bond.

For the sake of comparison, additional calculations were performed to estimate the strength of the O_2···His64 interaction. It is commonly accepted that His64 is protonated at N_ϵ in MbO_2 (Phillips and Schoenborn, 1981). Hence, our calculations were performed on the His93-heme-CO-His64 arrangement of protein structure II (CO···H-N_ϵ, in Fig. 3) after replacement of the CO by O_2 and setting the initial Fe-O-O angle to 180°. The linear Fe-O-O bond rapidly evolved toward its characteristic bent conformation (Rovira et al., 1997). Interestingly, the bending of O_2 took place over the same porphyrin quadrant as is found in the MbO_2 neutron structure (Phillips and Schoenborn, 1981). Fig. 4 shows the corresponding optimized structure. The O_2 bends in a direction away from His64, which indicates that steric interaction with His64 precludes the oxygen bending toward the His64. As a consequence of the hydrogen bond with His64, the final optimized FeOO angle (124°) is slightly larger than the optimized one for an isolated $FeP(Im)O_2$ model (122°). The strength of the O_2···His64 interaction amounts to −5.1 kcal/mol. (The recent study of Sigfridson and Ryde (1999) reported a larger difference between the binding energies for O_2 and CO (5.7 kcal/mol, whereas we found ~2 kcal/mol). This discrepancy is probably due to the different structures used: Sigridson and Ryde used the optimized structure of a heme model and an interacting imidazole, whereas we used QM/MM optimized structures taking into account the whole protein.) This value (−5.1 kcal/mol) should be regarded as a lower bound, as it is likely that the interaction would increase when using a His93-heme-O_2-His64 model extracted from a snapshot of a MbO_2 simulation. Overall, our results give support to arguments invoking the hydrogen bond with His64 as a factor responsible for the protein discrimination for CO.

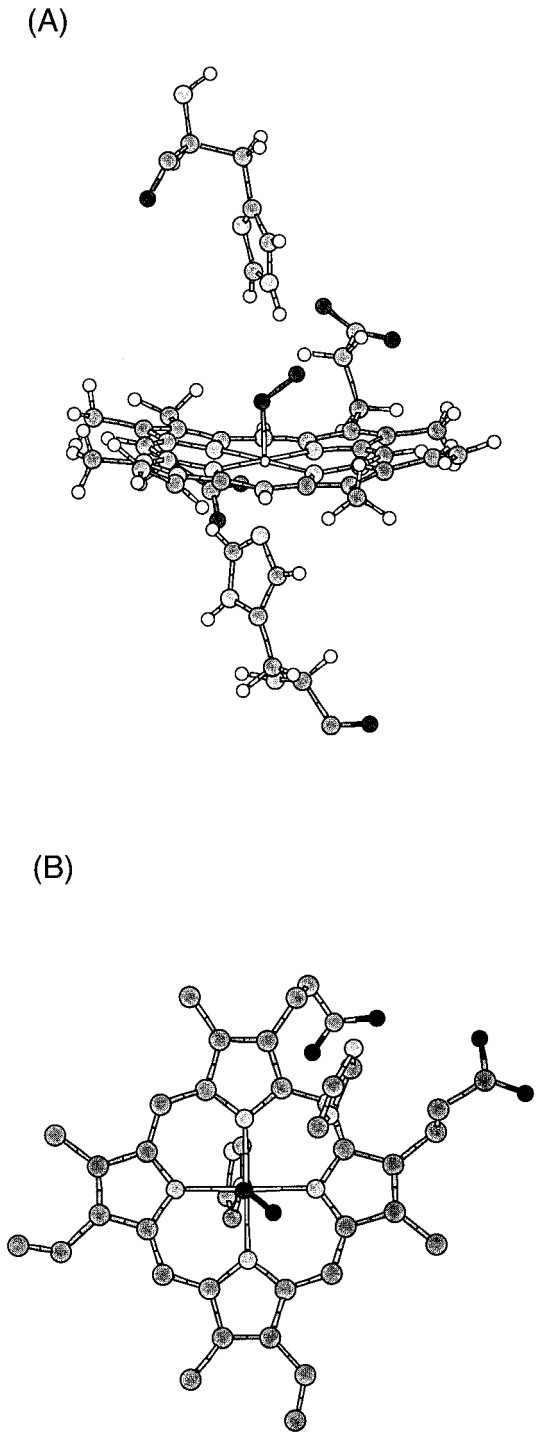

FIGURE 4 (*a*) His93-heme-CO-His64 fragment taken from the QM/MM optimized structure of oxymyoglobin, starting from the protein configuration II (Fig. 3); (*b*) Same structure viewed from top. The hydrogen atoms have been removed for clarity, and only the imidazole rings of His64 and His93 are kept.

CONCLUSIONS

In the present work we have performed hybrid QM/MM calculations based on density functional theory combined with the CHARMM force field to highlight the effect of the distal pocket conformation on the properties of the Fe-CO bond in MbCO and to help in the interpretation of the CO absorption bands in the IR spectra (the A states).

The neutron diffraction structure of MbCO, as well as selected snapshots from previous MD simulations using the CHARMM force field (Schulze and Evanseck, 1999), were used as initial structures. These structures were chosen to cover all possible changes in the rotational and tautomerization state of the highly mobile His64 residue. In all cases considered, the local structure around the Fe atom practically recovers that of the gas-phase heme-CO system, where the FeCO angle is linear. Even for the much smaller pocket given by the neutron diffraction structure, the deformation of the FeCO angle is marginal ($\leq 11°$). Therefore, the heme-CO structure seems to be quite robust, and the FeCO distortion cannot account for the observed IR absorptions.

Unlike the structure, the CO stretch frequency and the strength of the CO···His64 interaction appear to be very dependent on the orientation and tautomerization state of His64. Our calculations show that the CO···N_ϵ interaction upshifts the CO stretch frequency with respect to that of an unperturbed heme-CO model, for the two protein configurations considered. In contrast, the CO···H-N_ϵ interaction largely downshifts the CO frequency. The shift is practically zero when His64 is far from CO, in agreement with mutagenesis experiments showing an enhancement of A_0 when His64 is replaced for an apolar residue (Braunstein et al., 1993; Li et al., 1994). We found that the changes in ν_{CO} originate mainly from the position of the His64 residue, being independent of the position of the other protein residues, and can be rationalized in terms of the changes in the Fe-CO back-bonding when a positive/negative charged group approaches the CO ligand.

The energy of the CO···His64 interaction (≤ -3.4 kcal/mol) is related to the changes in $\Delta\nu_{CO}$: the interaction becomes more attractive as $\Delta\nu_{CO}$ increases. The energy of the CO···His64 interaction is lower than that of the O_2···His64 interaction (-5.1 kcal/mol).

Our calculations show that the CO···N_ϵ type interaction does not correspond to any of the absorptions of the IR spectra of MbCO, whereas the CO···H-N_ϵ type of interaction is the origin of the A_1, A_3 states. The small value of the frequency shift obtained for the corresponding rotated conformation (IV in Fig. 3) indicates that this conformation could also contribute to the A_0 and A_x absorptions, which are the less populated at normal pH. Taking into account that the time scale for substate interconversion is much shorter than that for tautomerization, our calculations suggest that His64 is protonated at N_ϵ in MbCO.

We thank the Garching Computer Center (Garching, Germany) for computing support. C. Rovira acknowledges the financial support of the "Incorporación de doctores y tecnólogos" program of the Spanish Ministry of Science and Technology. We thank Jürg Hutter for many useful discussions.

REFERENCES

Ansari, A., J. Berendzen, D. Braunstein, B. R. Cowen, H. Frauenfelder, M. K. Hong, E. T. Iben, J. B. Johnson, P. Ormos, T. B. Sauke, R. Scholl, A. Schulte, P. J. Steinbach, J. Vittitow, and R. D. Young. 1987. Rebinding and relaxation in the myoglobin pocket. *Biophys. Chem.* 26: 337–355.

Bhattacharya, S., S. F. Sukits, K. L. MacLaughlin, and J. T. J. Lecomte. 1997. The tautomeric state of histidines in myoglobin. *Biophys. J.* 73:3230–3240.

Becke, A. D. 1986. Density functional calculations of molecular bond energies. *J. Chem. Phys.* 84:4524–4529.

Braunstein, D. P., K. Chu, K. D. Egeberg, H. Frauenfelder, J. R. Mourant, G. U. Nienhaus, P. Ormos, S. G. Sligar, B. A. Springer, and R. D. Young. 1993. Ligand binding to heme proteins. III. FTIR studies of His-E7 and Val-E11 mutants of carbonmonoxymyoglobin. *Biophys. J.* 65:2447–2454.

Car, R., and M. Parrinello. 1985. Unified approach for molecular dynamics and density-functional theory. *Phys. Rev. Lett.* 55:2471–2474.

Cheng, X., and B. P. Schoenborn. 1991. Neutron diffraction study of carbonmonoxymyoglobin. *J. Mol. Biol.* 220:381–399.

Collman, J. P. 1997. Functional analogs of heme protein active sites. *Inorg. Chem.* 36:5145–5155.

Cui, Q., and M. Karplus. 2000. Molecular properties from combined QM/MM methods. I. Analytical second derivative and vibrational calculations. *J. Chem. Phys.* 112:1133–1149.

Frauenfelder, H., N. A. Alberding, A. Ansari, D. Braunstein, B. R. Cowen, M. K. Hong, I. E. T. Iben, J. B. Johnson, S. Luck, M. C. Marden, J. R. Mourant, P. Ormos, L. Reinisch, R. Scholl, A. Schu1te, E. Shyamsunder, L. B. Sorenson, P. J. Steinbach, A. Xie, R. D. Young, and K. T. Yue. 1990. Proteins and pressure. *J. Phys. Chem.* 94:1024–1038.

Frauenfelder, H., S. G. Sligar, and P. G. Wolynes. 1991. The energy landscapes and motions of proteins. *Science.* 254:1598–1603.

Fuchsman, W. H., and C. A. Appleby. 1979. CO and O_2 complexes of soybean leghemoglobins: pH effects upon infrared and visible spectra: comparison with CO and O_2 complexes of myoglobin and hemoglobin. *Biochemistry.* 18:1309–1321.

Galli, G., and M. Parrinello. 1991. Computer Simulation in Materials Science. V. Pontikis and M. Meyer, editors. Kluwer, Dordrecht, The Netherlands.

Havlin, R. H., N. Godbout, R. Salzmann, M. Wojdelski, W. Arnold, W., C. E. Schulz, and E. Oldfield. 1998. An experimental and density functional investigation of iron-57 Mössbauer quadrupole splittings in organometallic and heme-model compounds: applications to carbonmonoxy-heme protein structure. *J. Am. Chem. Soc.* 120:3144–3151.

Hong, M. K., D. Braunstein, B. R. Cowen, H. Frauenfelder, I. E. T. Iben, J. R. Mourant, P. Ormos, R. Scholl, A. Schulte, P. J. Steinbach, A. H. Xie, and R. D. Young. 1990. Conformational substates and motions in myoglobin: external influences on structure and dynamics. *Biophys. J.* 58:429–436.

Iben, I. E. T., D. Braunstein, W. Doster, H. Frauenfelder, M. K. Hong, J. B. Johnson, S. Luck, P. Ormos, A. Schulte, P. J. Steinbach, A. H. Xie, and R. D. Young. 1989. Glassy behavior of a protein. *Phys. Rev. Lett.* 62:1916:1919.

Johnson, J. B., D. C. Lamb, H. Frauenfelder, J. D. Müller, B. McMahon, G. U. Nienhaus, and R. D. Young. 1996. Ligand binding to heme proteins. VI. Interconversion of taxonomic substates in carbonmonoxymyoglobin. *Biophys. J.* 71:1563–1573.

Kachalova, G. S., A. N. Popov, and H. D. Bartunik. 1999. A steric mechanism for inhibition of CO binding to heme proteins. *Science.* 284:473–476.

Kuriyan, J., S. Wilz, M. Karplus, and G. A. Petsko. 1986. X-ray structure refinement of carbon-monoxy-Fe(II)-myoglobin at 1.5 Å. *J. Mol. Biol.* 192:133–154.

Kushkuley, B., and Starov. 1997. Theoretical study of the electrostatic and steric effects on the spectroscopic characteristics of the metal-ligand unit of heme proteins. II. C-O vibrational frequencies, ^{17}O isotropic chemical shifts, and nuclear quadrupole coupling constants. *Biophys. J.* 72: 899–912.

Li, T., M. L. Quillin, G. N. Phillips, and J. S. Olson. 1994. Structural determinants of the stretching frequency of CO bound to myoglobin. *Biochemistry.* 33:1433–1446.

Lim, M., T. A. Jackson, and P. A. Anfinrud. 1995. Binding of CO to myoglobin from a heme pocket docking site to form nearly linear Fe-C-O. *Science.* 269:962–966.

Louie, S. G., S. Froyen, and M. L. Cohen. 1982. Nonlinear ionic pseudopotentials in spin-density-functional calculations. *Phys. Rev. B.* 26: 1738–1742.

Olson, J. S., and G. N. Phillips. 1996. Kinetic pathways and barriers for ligand binding to myoglobin. *J. Biol. Chem.* 271:17593–17596.

MacKerell, A., D. Bashford, M. Bellott, R. L. Dunbrack, J. D. Evanseck, M. J. Field, J. Gao, H. Guo, S. Ha, D. Joseph, L. Kuchnir, K. Kuczera, F. T. K. Lau, C. Mattos, S. Michnick, D. T. Nguyen, T. Ngo, B. Prodhom, W. E. Reiher, B. Roux, M. Schlenkrich, J. Smith, R. Stote, J. Straub, M. Watanabe, J. Wiorkiewicz-kuczera, D. Yin, and M. Karplus. 1998. All atom empirical potential for molecular modeling and molecular dynamics studies of proteins. *J. Phys. Chem. B.* 102:3586–3616.

Morikis, D., P. M. Champion, B. A. Springer, and S. G. Sligar. 1989. Resonance Raman investigations of site-directed mutants of myoglobin: effects of distal histidine replacement. *Biochemistry.* 28:4791–4800.

Mourant, J. R., D. Braunstein, K. Chu, H. Frauenfelder, G. U. Nienhaus, P. Ormos, and R. D. Young. 1993. Ligand binding to heme proteins. II. Transitions in the heme pocket of myoglobin. *Biophys. J.* 65: 1496–1507.

Nienhaus, G. U., and R. D. Young. 1996. Protein dynamics. *In* Encyclopedia of Applied Physics, Vol. 15. G. L. Trigg, editor. VCH Publishers, New York.163–184.

Nienhaus, G. U., J. D. Müller, B. H. McMahon, and H. Frauenfelder. 1997. Exploring the conformational energy landscape of proteins. *Phys. D.* 107:297–311.

Oldfield, E., Augspurger, J. D., and C. E. Dykstra. 1991. A molecular model for the major conformational substates in heme proteins. *J. Am. Chem. Soc.* 113:7537–7541.

Perdew, J. P. 1986. Density-functional approximation for the correlation energy of the inhomogeneous electron gas. *Phys. Rev. B.* 1986:33: 8822–8824.

Phillips, S. E. V., and B. P. Schoenborn. 1981. Neutron diffraction reveals oxygen-histidine hydrogen bond in oxymyoglobin. *Nature.* 292:81–82.

Phillips, G. N., M. L. Teodoro, T. L. I., B. Smith, and J. S. Olson. 1999. Bound CO is a molecular probe of electrostatic potential in the distal pocket of myoglobin. *J. Phys. Chem. B.* 103:8817–8829.

Ray, G. B., X.-Y. Li, J. A. Ibers, J. L. Sessler, and T. G. Spiro. 1994. How far proteins bend the FeCO unit? Distal polar and steric effects in heme proteins and models. *J. Am. Chem. Soc.* 116:162–176.

Röthlisberger, U., P. Carloni, K. Doclo, and M. Parrinello. 2000. A comparative study of galactose oxidase and active site analogs based on QM/MM Car-Parrinello simulations. *J. Biol. Inorg. Chem.* 5:236–250.

Rovira, C., K. Kunc, J. Hutter, P. Ballone, and M. Parrinello. 1997. Equilibrium geometries and electronic structure of iron-porphyrin complexes: a density functional study. *J. Phys. Chem. A.* 101: 8914–8925.

Rovira, C., and M. Parrinello. 1999. Factors influencing ligand binding properties of heme models: a first principles study of picket-fence and protoheme complexes. *Chem. Eur. J.* 5:250–262.

Rovira, C., and M. Parrinello. 2000. Harmonic and anharmonic dynamics of Fe-CO and Fe-O_2 in heme models. *Biophys. J.* 78:93–100.

Sage, J. T., and P. M. Champion. 1996. Small substrate recognition in heme proteins. *In* Comprehensive Supramolecular Chemistry, Vol. 5. K. S. Suslick, editor. Pergamon, Oxford, UK.171–213.

Sage, J. T., and W. Jee. 1997. Structural characterization of the myoglobin active site using infrared crystallography. *J. Mol. Biol.* 274:21–26.

Schulze, B. 1999. Theoretical assessment of global and local motions in carbonmonoxy myoglobin and their functional significance. Ph.D. Thesis. University of Miami, Miami, FL.

Schulze, B., and J. D. Evanseck. 1999. Cooperative role of Arg45 and His64 in the spectroscopic A_3 state of carbonmonoxy myoglobin: molecular dynamics simulations, multivariant analysis, and quantum mechanical computations. *J. Am. Chem. Soc.* 121:6444–6454.

Shimada, H., and W. S. Caughey. 1982. Dynamic protein structures. *J. Biol. Chem.* 257:11893–11900.

Sigfridson, E., and U. Ryde. 1999. On the significance of hydrogen bonds for the discrimination between CO and O_2 by myoglobin. *J. Biol. Inorg. Chem.* 4:99–110.

Slebodnick, C., and J. A. Ibers. 1997. Myoglobin models and steric origins of the discrimination between O_2 and CO. *J. Biol. Inorg. Chem.* 2:521–525.

Spiro, T. G., and P. M. Kozlowski. 1998. Discordant results on FeCO deformability in heme proteins reconciled by density functional theory. *J. Am. Chem. Soc.* 120:4524–4525.

Springer, B. A., S. G. Sligar, J. S. Olson, and G. N. Phillips. 1994. Mechanisms of ligand recognition in myoglobin. *Chem. Rev.* 94: 699–714.

Stryer, L. 1995. Biochemistry, 4th ed. Freeman, New York.

Troullier, N., and J. L. Martins. 1991. Efficient pseudopotentials for plane-wave calculations. *Phys. Rev. B.* 43:1993.

Vangberg, T., D. F. Bocian, and A. Ghosh. 1997. Deformability of Fe(II)CO and Fe(III)CN groups in heme protein models: nonlocal density functional theory calculations. *J. Biol. Inorg. Chem.* 2:526–530.

Vojtechovsky, J., K. Chu, J. Berendzen, R. M. Sweet, and I. Schlichting. 1999. Crystal structures of myoglobin-ligand complexes at near-atomic resolution. *Biophys. J.* 77:2153–2174.

Unno, M., J. F. Christian, J. S. Olson, J. T. Sage, and P. M. Champion. 1998. Evidence for hydrogen bonding effects in the iron ligand vibrations of carbonmonoxy myoglobin. *J. Am. Chem. Soc.* 120:2670–2671.

Yang, F., and G. N. Phillips. 1996. Crystal structures of CO-deoxy- and met-myoglobins at various pH values. *J. Mol. Biol.* 256:762–774.

Zhu, L., J. T. Sage, A. A. Rigos, D. Morikis, and P. M. Chempion. 1992. Conformational interconversion in protein crystals. *J. Mol. Biol.* 224: 207–215.